X-713-67-194

NASA TM X- 55773

SPECTRAL RESPONSE MEASURMENTS OF SOLAR CELLS

GPO PRICE $ _____

CFSTI PRICE(S) $ _____

Hard copy (HC) 3.00

Microfiche (MF) .65

ff 653 July 65

APRIL 1967

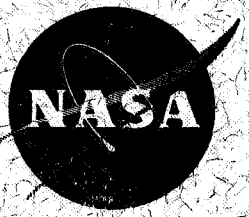

GODDARD SPACE FLIGHT CENTER

GREENBELT, MARYLAND

X-713-67-194

SPECTRAL RESPONSE MEASUREMENTS OF SOLAR CELLS

Contract No. NAS5-3743

William G. Gdula

Prepared by

Electro-Mechanical Research, Inc.
Aerospace Sciences Division
College Park, Maryland

for

GODDARD SPACE FLIGHT CENTER
Greenbelt, Maryland

TABLE OF CONTENTS

ILLUSTRATIONS

TABLES

SPECTRAL RESPONSE MEASUREMENTS OF SOLAR CELLS

INTRODUCTION

In consideration of the importance from both the fundamental viewpoint and practical application of the spectral response measurements of photovoltic devices, particularly solar cells, a considerable effort has been expended to develop the necessary electro-optic instrumentation required for accurate measurements. In addition, the capability of predicting operating performance characteristics and deriving physical material parameters which are closely related to final performance features, has been refined so that experimental analysis is performed on a routine basis.

An outline of the instrumentation description is presented along with experimental results and applications.

SPECTRAL RESPONSE MEASUREMENT INSTRUMENTATION

General instrumentation requirements for measuring the quantum yields of photovoltaic devices include a monochromator with a constant bandwidth function and a high transmission efficiency in the wavelength regions of the device response. A 1 meter focal-length grating monochromator made by McPherson Instruments and the necessary rationing electronics comprises the present system along with the external beam splitting and transfer optics. The complete schematic of the optical layout is included in Figure 1. An absolute spectral reflectance integrating sphere has been added to the monochromator which allows the concurrent measurement of the solar cell surface reflectance properties. Figure 2 shows the complete system.

The grating monochromator is a Czerny turner design and includes a 3" x 3" B & L grating blazed at 4000 A° with 600 lines per mm. Maximum slit resolution obtainable is 0.3A°. As seen from Figure 1, the monochromatic beam is divided by a front-surfaced wedge chopping assembly with the incident beam alternately directed to the sample surface and a Reeder blackbody detector at a rate of 6.66 cps.

A Brower synchronous rationing system outlined in Figure 3 enables the solar cell monochromatic short-circuit current to be divided by the monochromatic photon intensity which is measured by a blackbody type detector. The electronically ratioed output is recorded on an X-YY plotter in both and equal energy and/or equal photon density mode.

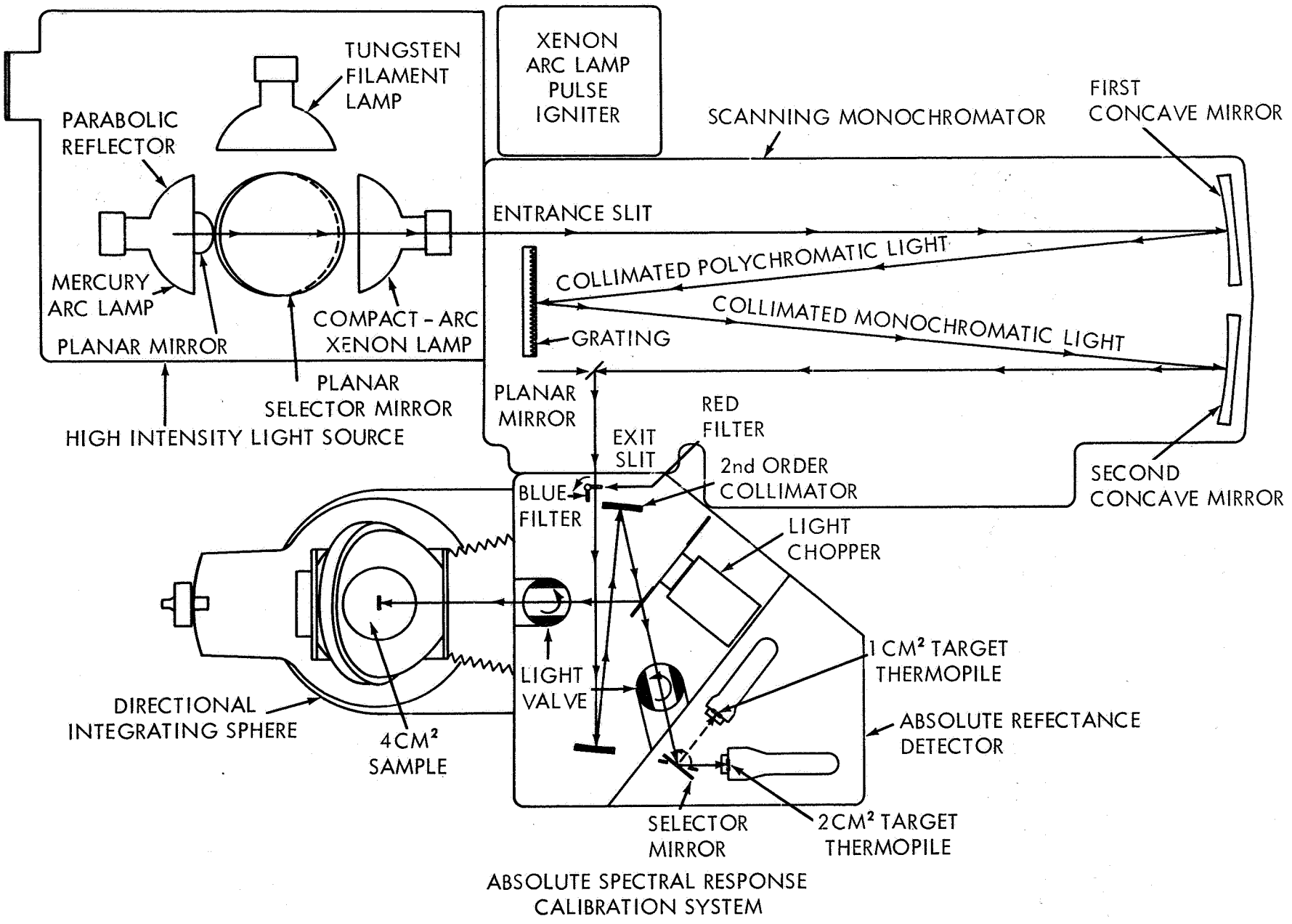

Figure 1. Absolute Spectral Response Calibration System

Figure 2. Pictural Layout of Measurement System

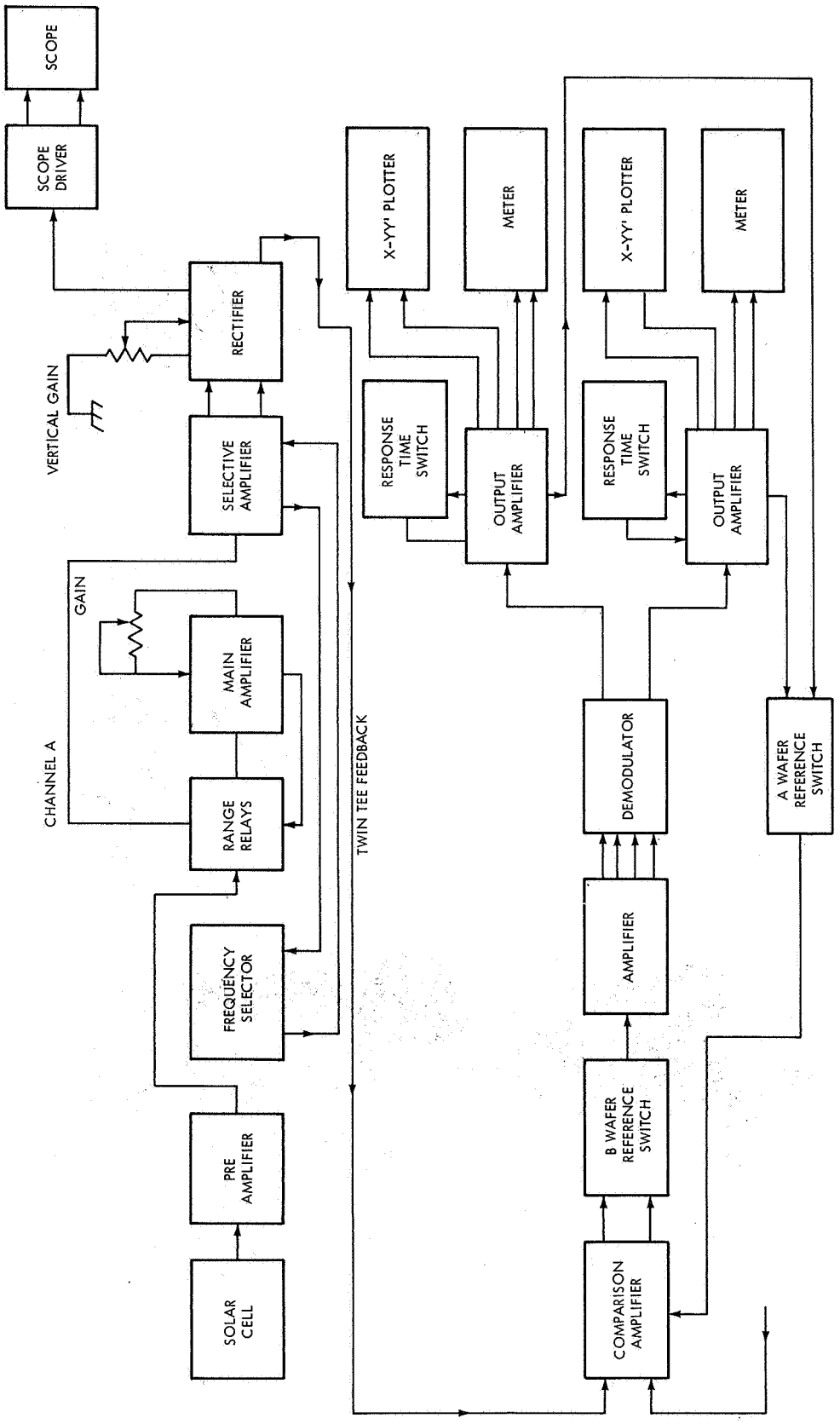

Figure 3. Synchronous Ratioing System

Signal flow of the basic electronics of the system is as follows. There are two identical channels, one for the solar cell input and one for the blackbody detector whose outputs are electronically ratioed in the comparison amplifier. The signal level generated by a solar cell when monochromatic energy is incident on the cell is transformer coupled to the input X200 pre-amp and subsequently undergoes attenuation through a front panel controlled antenuator network covering four decade levels. The three-stage nuvistor pre-amplifier is designed for low frequency response, stability and low input noise. All circuitry is isolated from the main chassis and the complete system ground is provided at the pre-amp input to avoid any possible ground loops. The chopped signal output after undergoing a feed-back stabilized gain of 200 is directed to a range relay network which provides the proper input level to the main amplifier. The main amplifier contains two D.C. coupled signal amplifiers; the first input presents a high impedance to prevent any loading effects in the range relay module and the second provides a low gain, impedance matching output. The output of the main amplifier is adjusted by a front panel variable gain control and is conditioned in a low frequency roll-off network before being applied to a fixed frequency selective amplifier. The frequency selector unit contains the phase delay capacitors which determine the coarse phasing of the chopped input signal in addition to the twin-tee network for the selective amplifier and all other tuned circuits which are dependent upon the light chopping frequency. At the center chopping frequency the selective amplifier has a gain of approximately 100 where the twin-tee filter in the feedback loop appears as an open-circuit. This amplifier is D.C. coupled throughout with the necessary stability being achieved through the twin-tee feedback path. Both normal-phase and paraphase outputs are generated in the selective amplifier for use in the synchronous rectifier module. The push-pull outputs are applied to high speed mercury-wetted relays in the rectifier module which are driven in synchronism with the light chopper to produce positive and negative full-wave rectified signals having D.C. components at the chopping frequency; low pass filters remove the ripple before application to a double-pole solid state chopper driven by sequential gates at approximately 1000 cps.

The final output of the solar cell channel is comprised of a chopped signal having positive and negative D.C. levels separated by equal spaces corresponding in time with the chopped signal from the thermocouple detector channel. If the ratio of the two separate channels, i.e. solar cell output referenced to the blackbody detector output is not required the ratio mode is bypassed and the instrument is used as two independent synchronous amplifiers. The chopped signals from the solar cell and detector modules are properly phased and added in the common comparison amplifier which ultimately provides two unique composite signal outputs. When the independent mode is selected the summed output from the comparison amplifier is applied to a fixed 50:1 attenuator before amplification in the X100 amplifier. Paraphase output signals from this amplification

stage are applied to the Demodulator where the composite signal is restored to the original two channel D.C. outputs. These separate signals representing the solar cell monochromatic response and the measured monochromatic photon intensity are then referred to the final output amplifiers which drive the panel meter and the external x-yy plotter. Wavelength calibration is derived from a linear function generation on the gear box of the monochrometer and is applied to the x-base of the plotter.

When the ratio mode is selected the amplitude of the one channel, the reference energy, is held constant by means of an automatic servo gain control; the signal of the other channel after demodulation now represents a true ratio relative to the reference signal. This ratio is achieved regardless of the signal level of the reference channel.

For some equal photon density applications and additional clarity of the performance features of the collection efficiency attribute of the p/n junction a quantum yield, equal photon density measurement, is desirable. This has been achieved by the addition of an operational amplifier and function generator stage added to the final output. The two channel channel capabilities of the plotter enables the quantum yield and spectral response or either one plus the reference ratioed output to be recorded as a function of wavelength. In addition, the grating monochromator has been programmed to operate from 3700 A° to 12000 A°, typical working regions of present day solar cells.

SYNCHRONIZATION

The importance of the initial synchronization in achieving the final accuracies of the instrumentation merits a brief summary of this system. A synchronization Block Diagram given in Figure 4 shows that the input square wave pulse derived from a photoconductive element modulated by a small secondary blade positioned on the main shaft of the chopper assembly provides the origin of synchronization The main trigger generator amplifies this pulse and also provides paraphase gates at the optical chopping frequency and generates positive trigger pulses at twice this frequency. Reference phase gates and a delayed trigger pulse are provided to the Fixed Delay and front panel phasing switches. The output from the Variable Delay in combination with a selected phase gate is applied to a flip-flop which generates the calibration and offset signals, the rectifier relay gates, horizontal sweep trigger and the main synchronizing output gates at the optical chopper frequency.

EXPERIMENTAL RESULTS

Solar cells with a diversity of spectral responses have been measured and the degree of accuracy in predicting the short-circuit current output has been

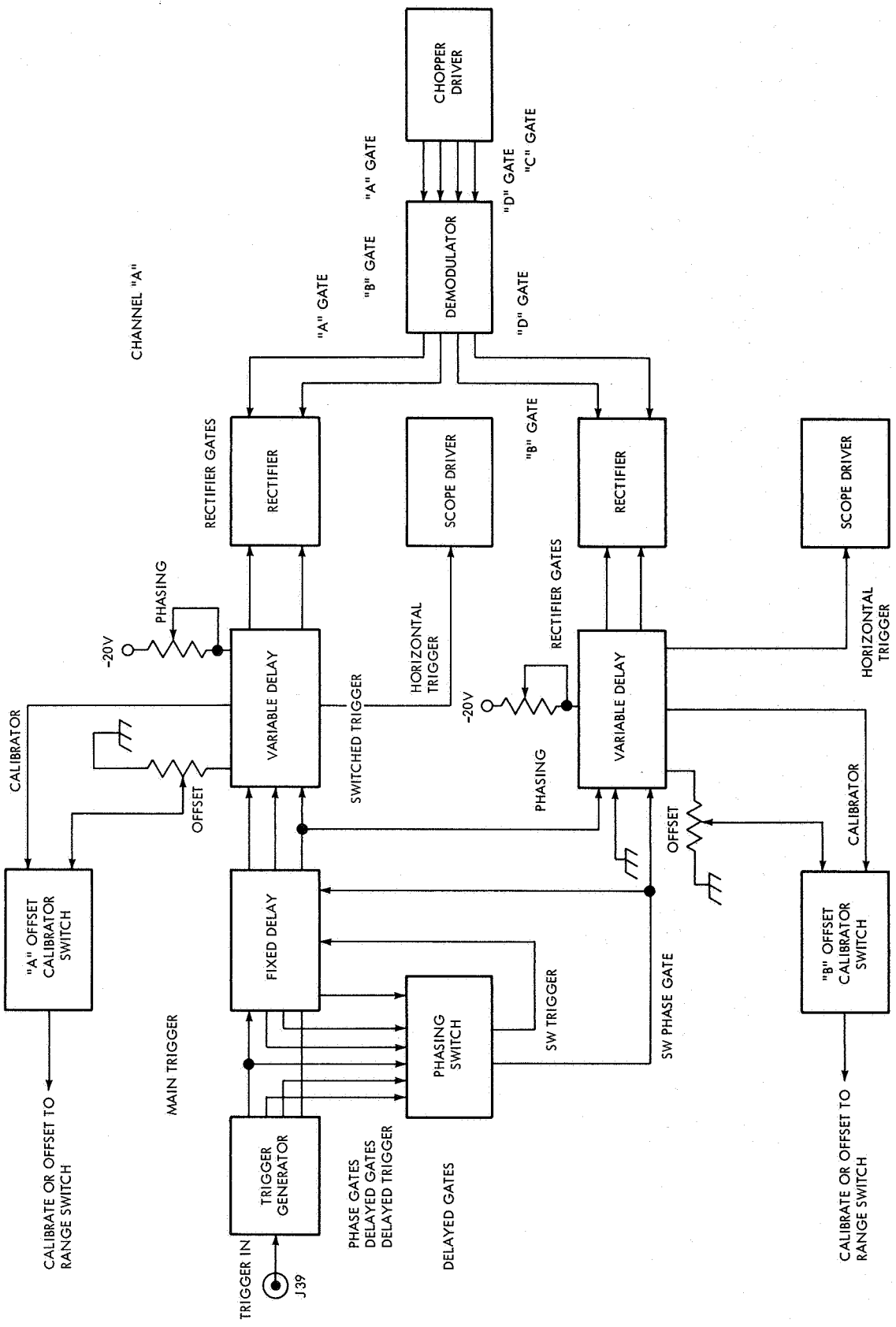

Figure 4. Synchronization Block Diagram

established. A procedure in calculating the output currents has been developed by using a flight calibrated cell at 47,000 feet as a standard. Accuracies obtained by this method are comparable to those when using the absolute calibration of a blackbody detector.

Spectral response measurements of silicon solar cells from eight manufacturers which typify their characteristics of production lots i.e., collection efficiency, surface reflectance and diode properties are shown in Figures 5 through 13. It is overtly apparent that there are large variations in the spectral responses of cells developed by the manufacturers. Table 1 gives the pertinent information of these cells and includes open-circuit voltage, conversion efficiency, short-circuit current measured under solar simulation conditions and calculated short-circuit currents from AMO solar irradiance using the NRL data. When comparing the calculated data with the measured solar cell short-circuit currents it is seen from Table 1 that calculated data agrees within ± 2.6% from the values obtained with the laboratory simulator adjusted to an energy level determined from cell measurements at 47,000 feet.

GENERAL THEORY

There have been numerous treatments of the theoretical aspects of the spectral response measurement with each essentially resolving into a solution of the continuity equation; essential differences in approach generally are variations in the boundary conditions and the selected physical parameters. A simplified treatment which still retains a clear physical insight to the phenomena is as follows. By use of Lamberts' absorption law a photon density incident on the solar cell surface is attenuated by the unique optical absorption coefficient α, of the material. In a homogeneous isotropic crystal a decrease of intensity amounting to the fraction $\Delta N_0/N$ of the initial photon density can be equated to the thickness X by the proportionality constant α. Thus,

$$\frac{\Delta N}{N} = -\alpha \Delta X \tag{1}$$

The negative sign signifies that the intensity has been reduced. Put in differential form and simple integration gives

$$\ln N = -\alpha X + \ln N_0 \tag{2}$$

and

$$N = N_0 \, e^{-\alpha X} \tag{3}$$

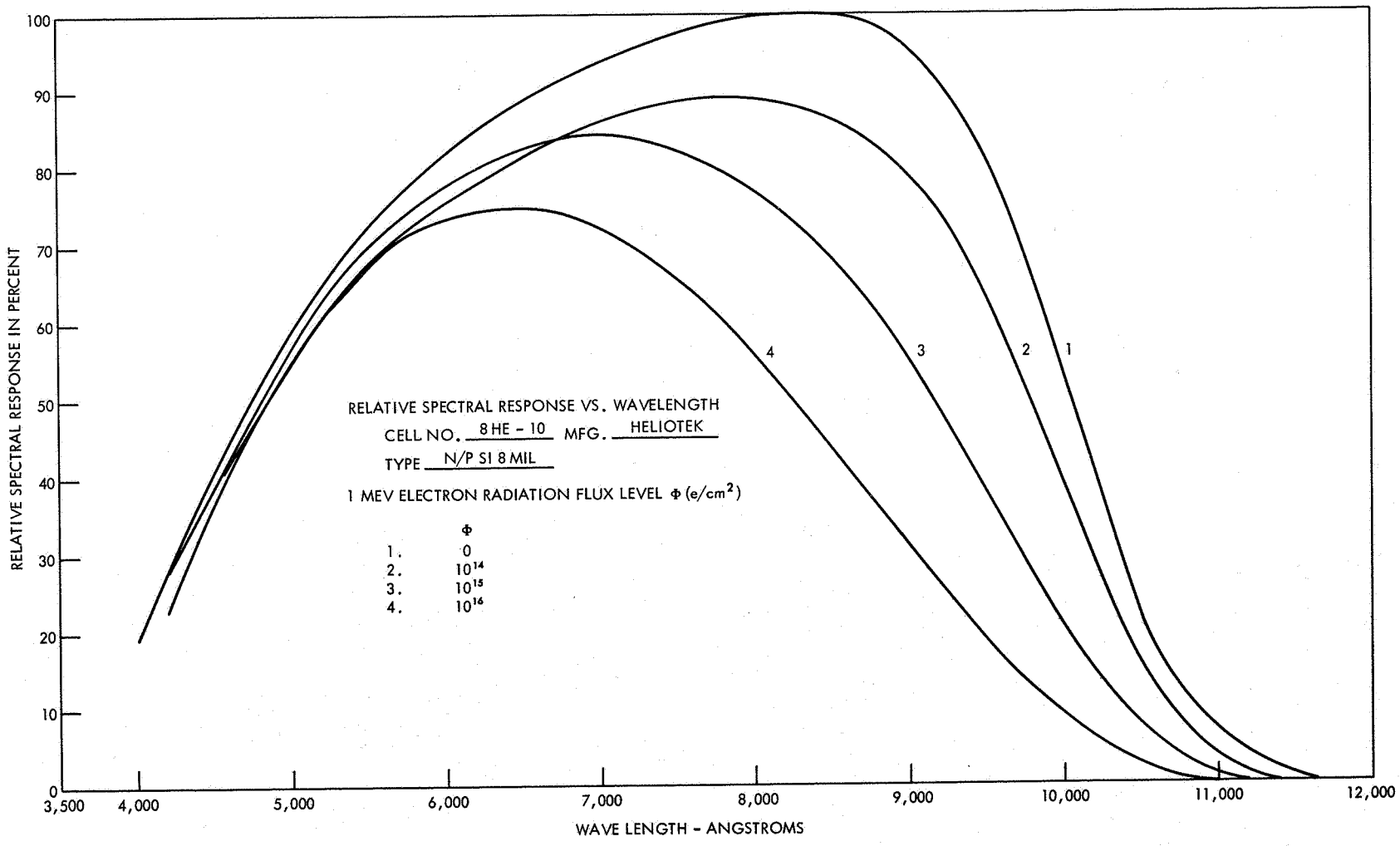

Figure 5. Solar Cell Spectral Responses

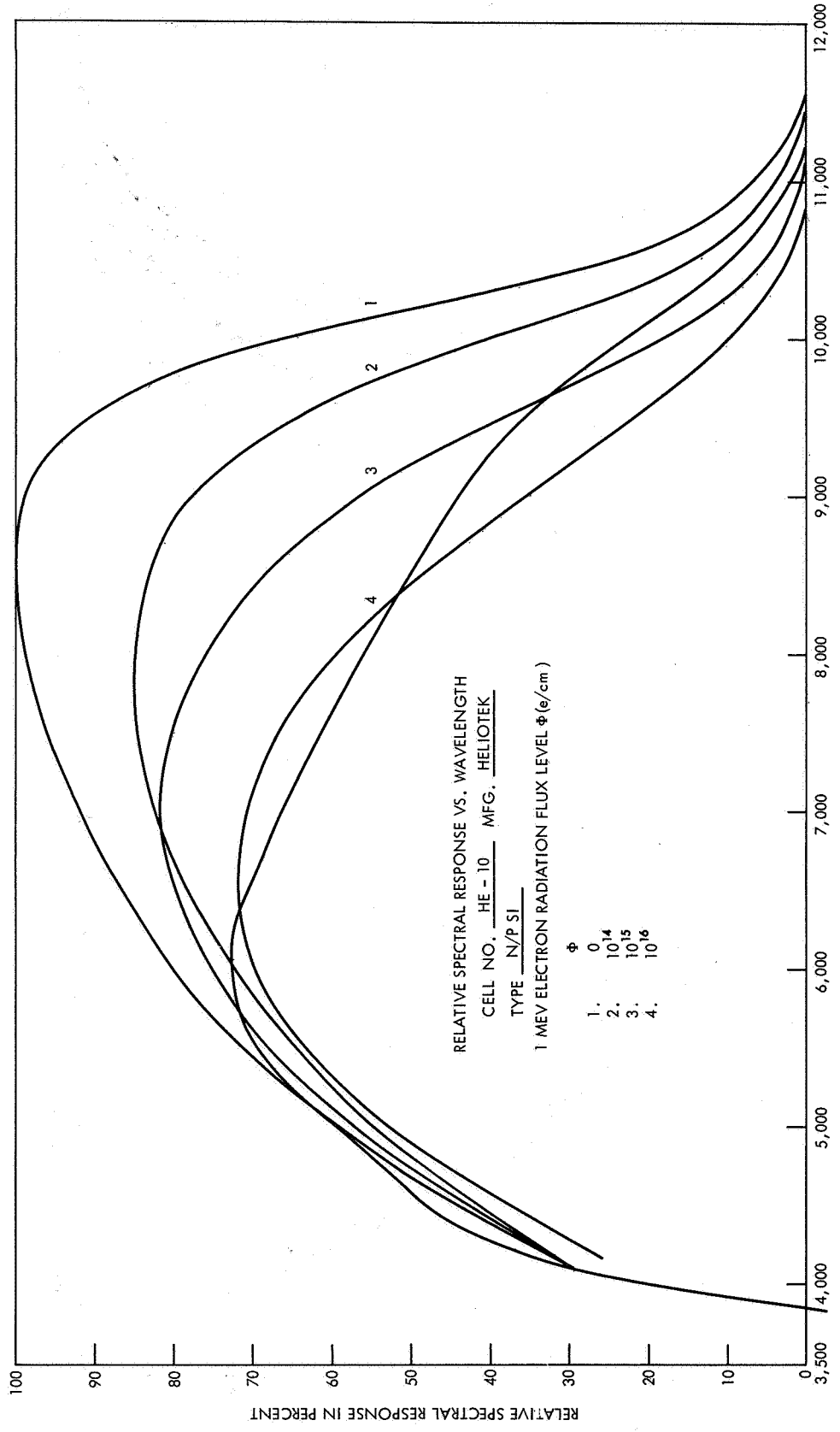

Figure 6. Solar Cell Spectral Responses

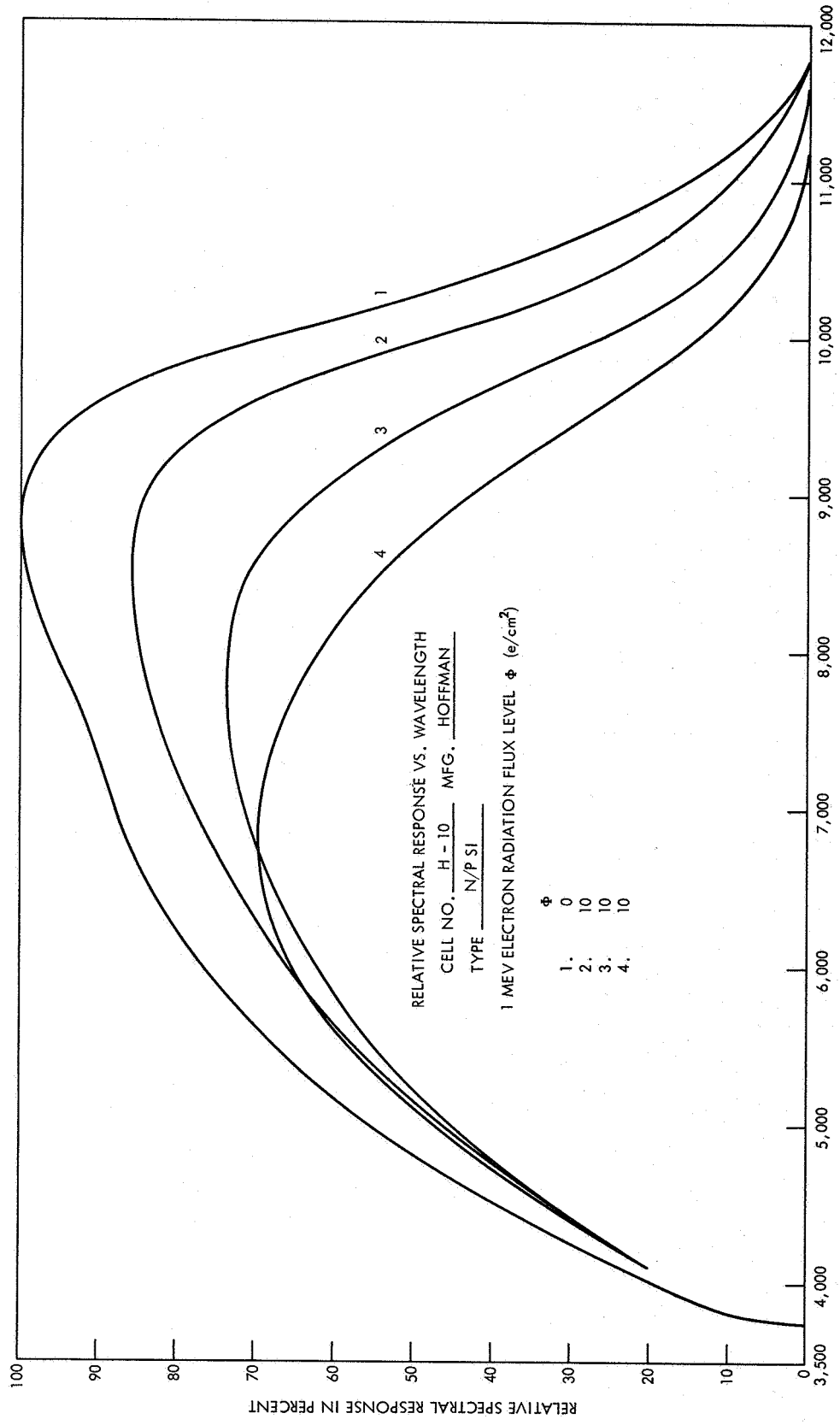

Figure 7. Solar Cell Spectral Responses

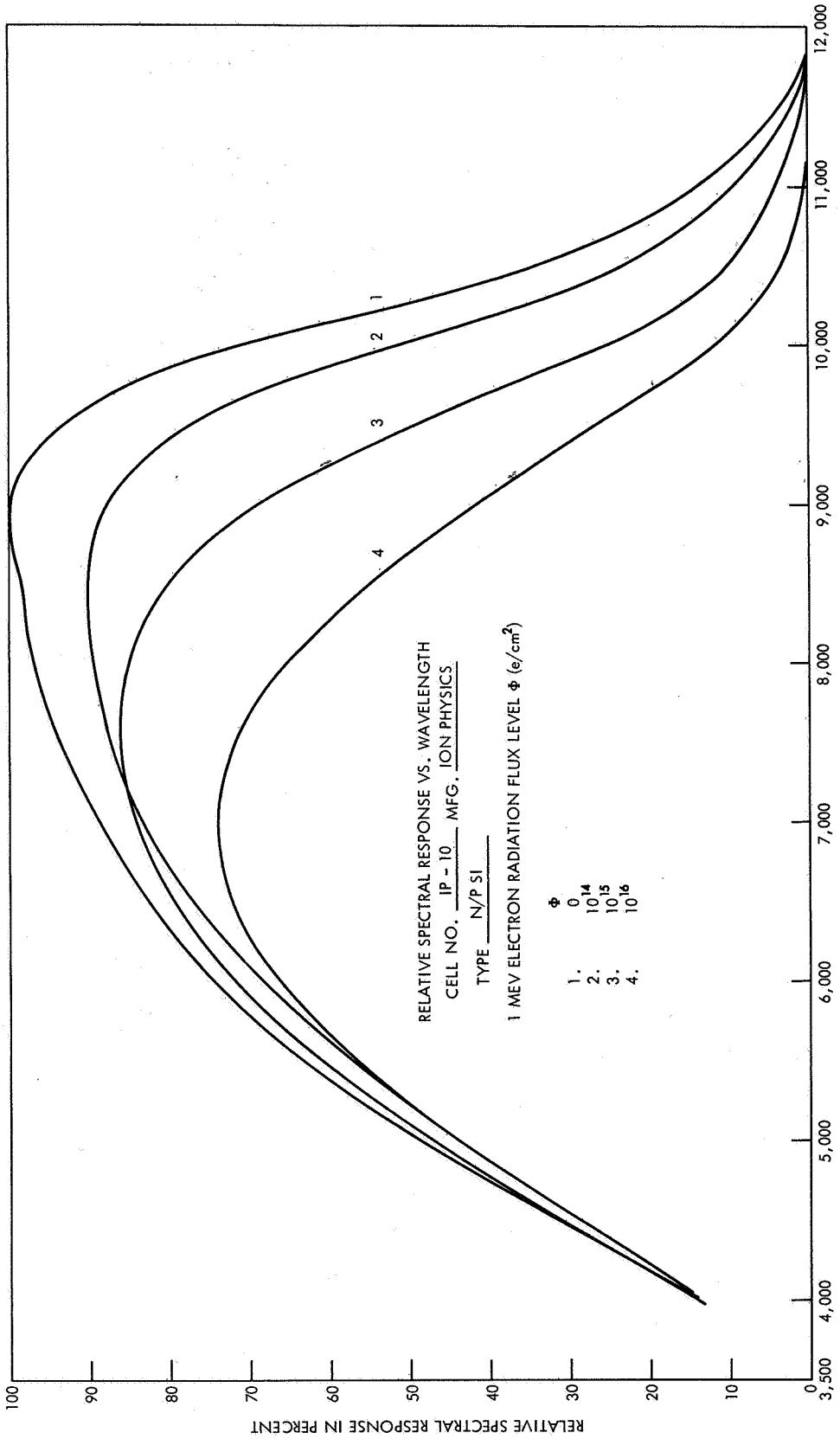

Figure 8. Solar Cell Spectral Responses

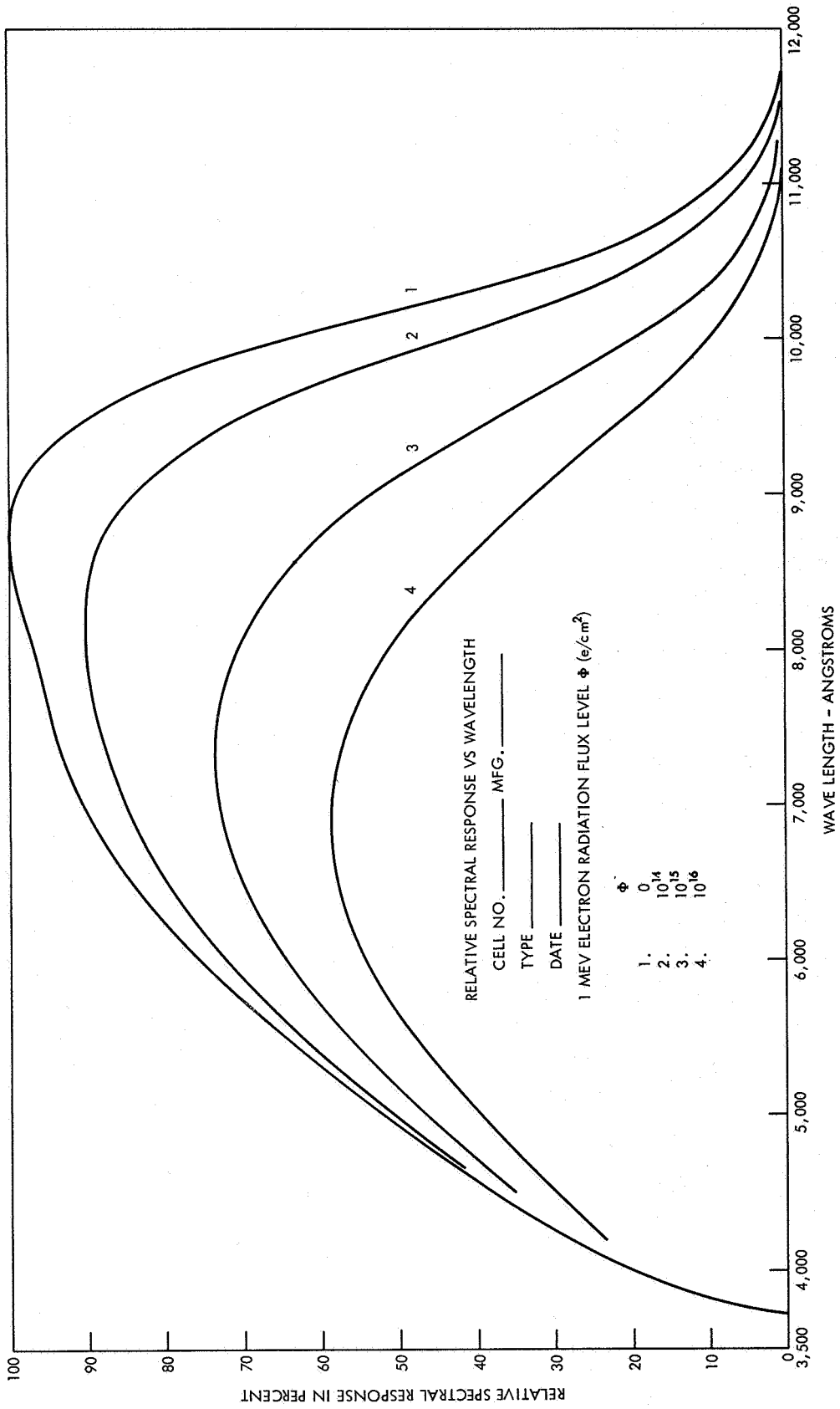

Figure 9. Solar Cell Spectral Responses

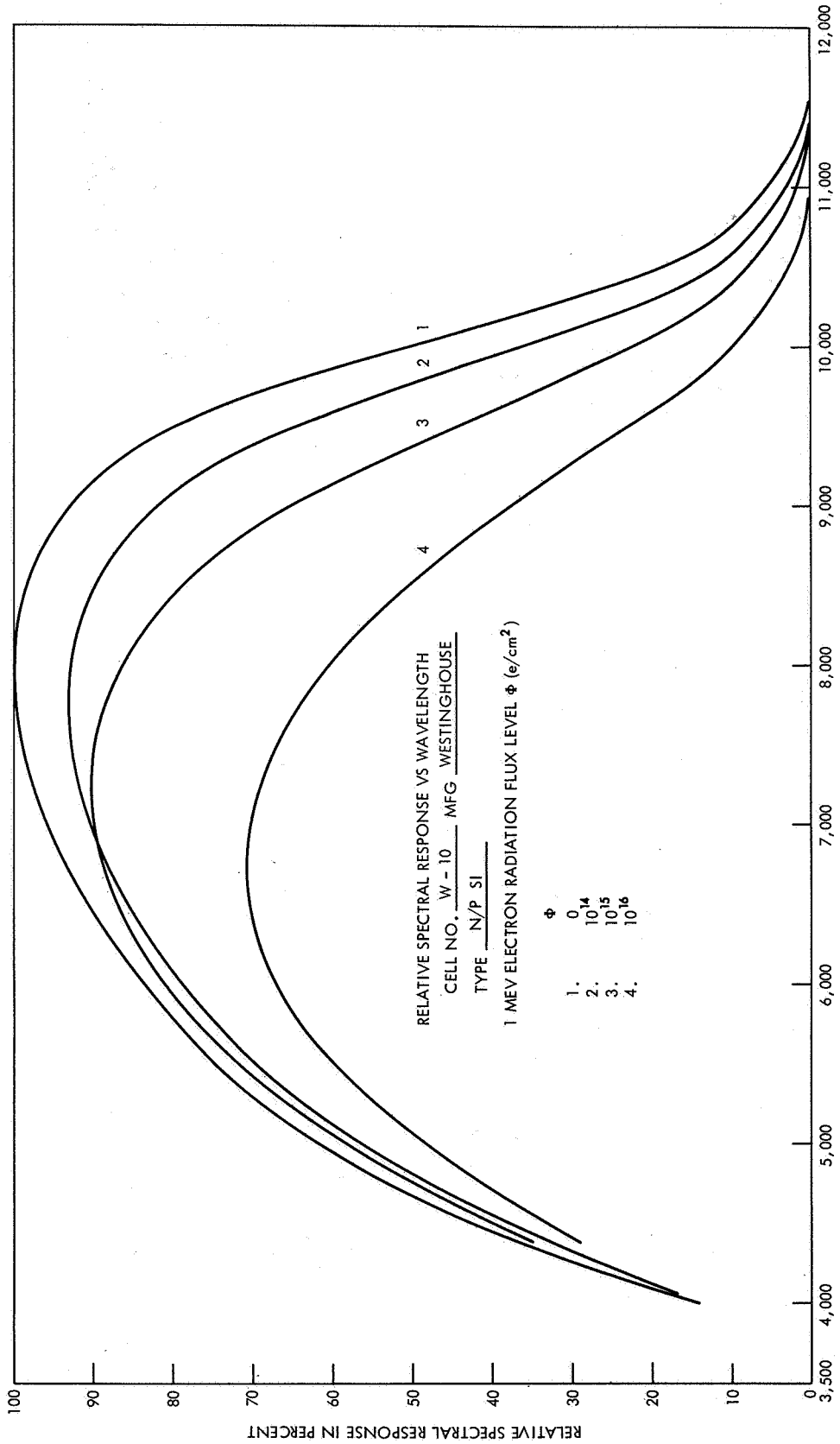

Figure 10. Solar Cell Spectral Responses

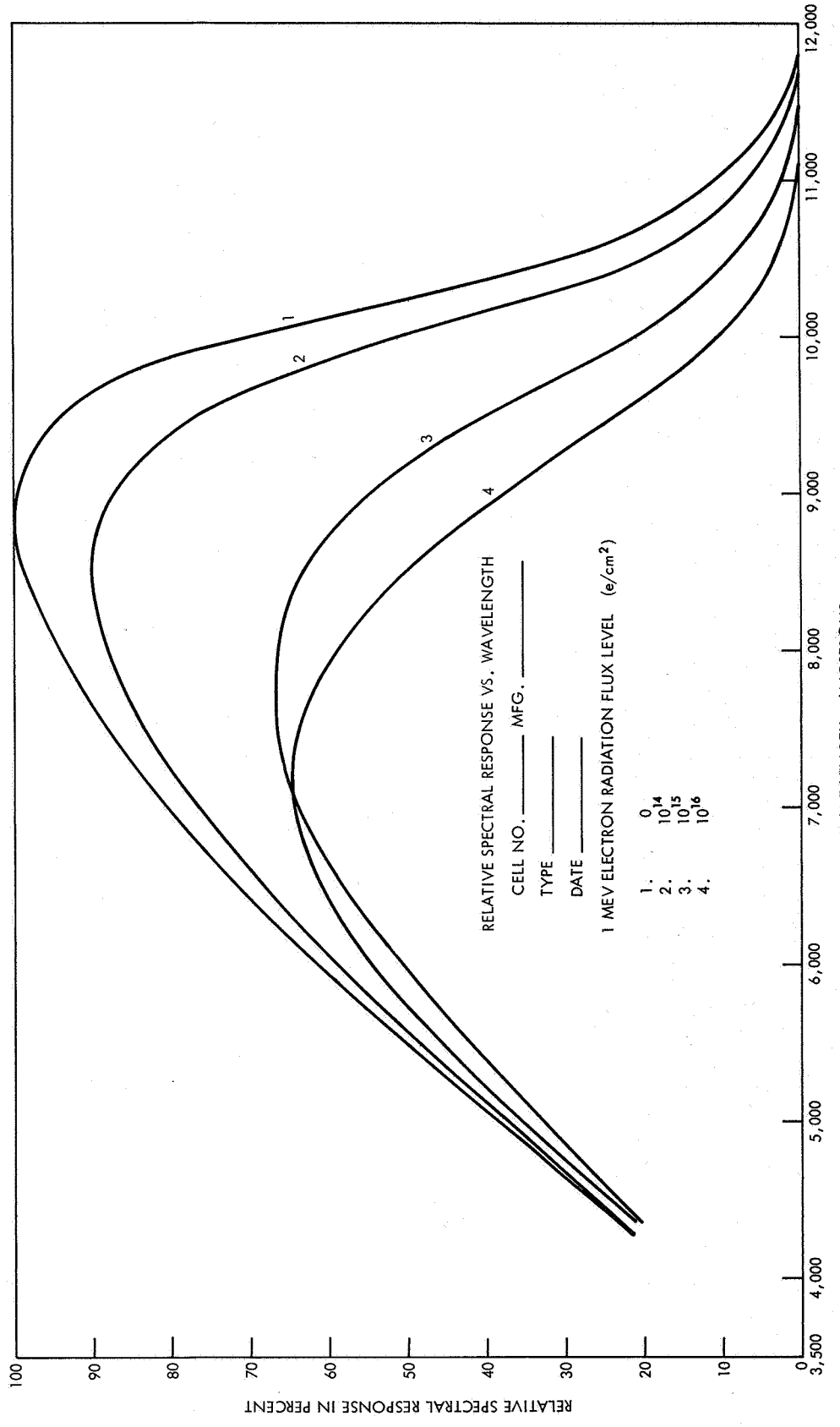

Figure 11. Solar Cell Spectral Responses

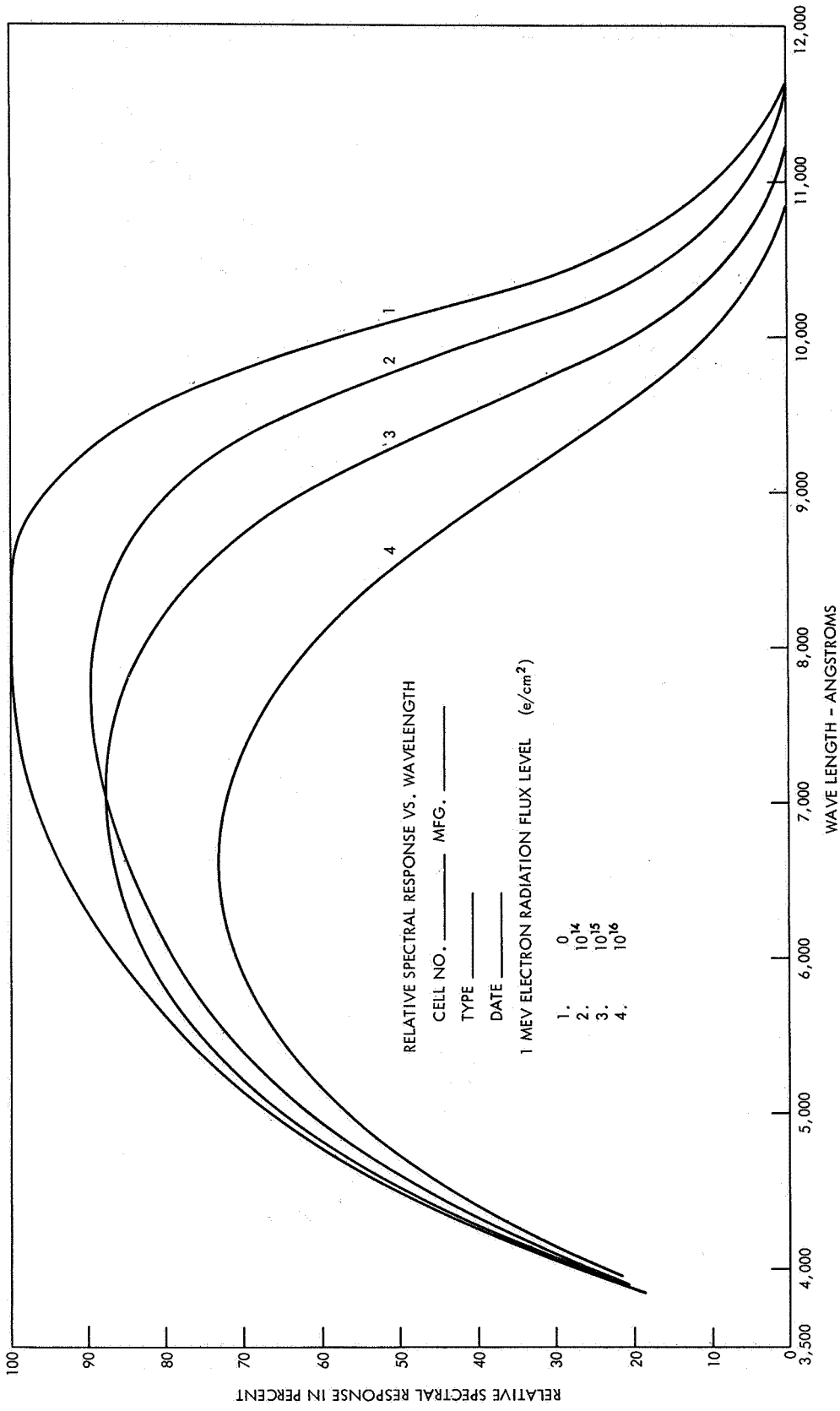

Figure 12. Solar Cell Spectral Responses

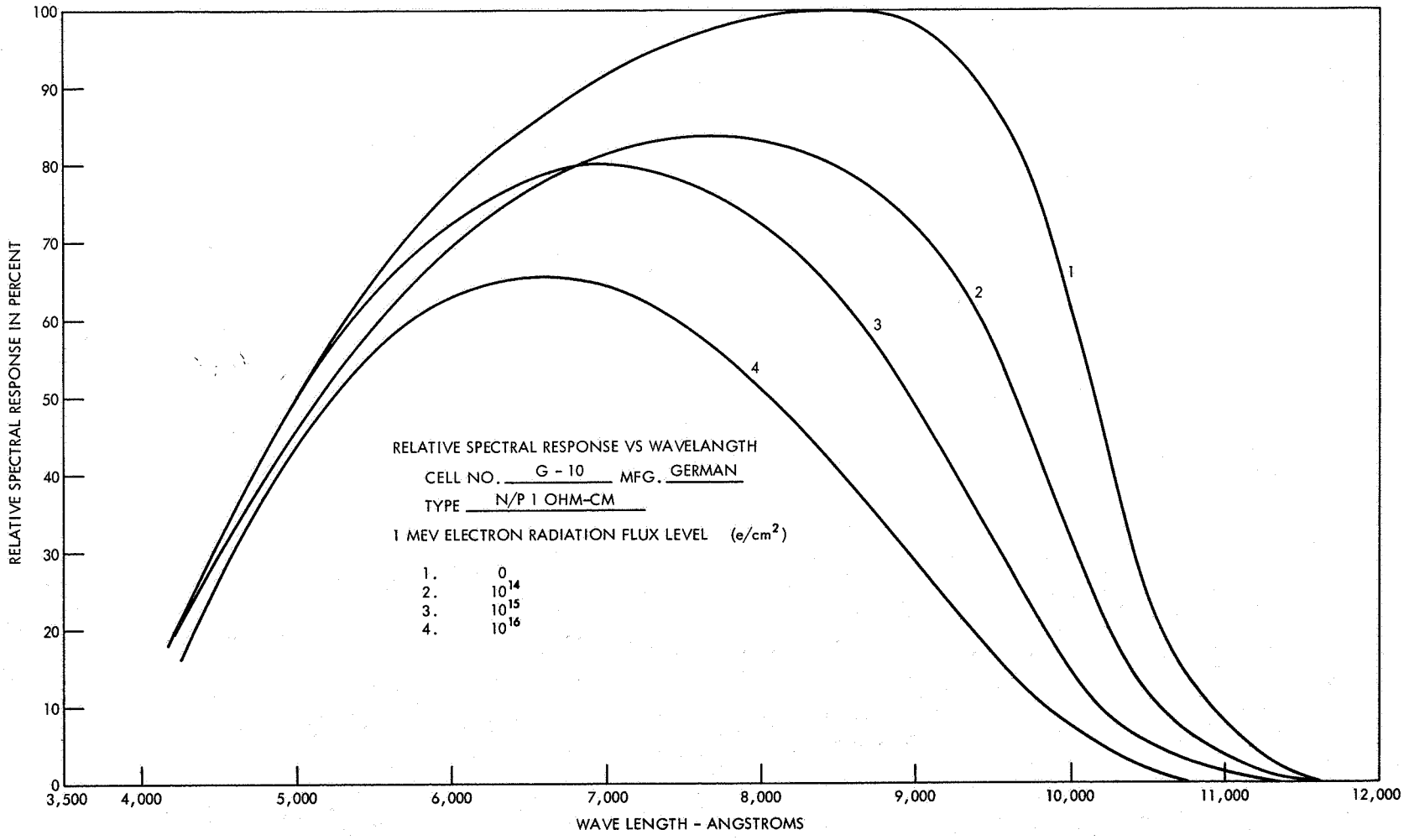

Figure 13. Solar Cell Spectral Responses

TABLE 1

CELL NO. MANUFACTURER	V_{oc}	η eff	I_{sc}	Calculated I_{sc}	Dev. %	
1. HELIOTEK	.557	10.9	72.6	73.8	+ 1.6	
2. HELIOTEK (8)	.578	10.2	63.0	64.7	+ 2.1	
3. HOFFMAN	.555	10.3	70.5	69.9	- 0.8	
4. ION PHYSICS	.550	9.1	62.7	61.4	- 2.3	
5. TEXAS INSTRUMENT	.545	10.3	73.6	74.2	+ 0.9	
6. WESTINGHOUSE	.535	8.3	61.6	63.1	+ 2.6	
7. BRITISH	.554	8.8	62.9	63.6	+ 1.2	
8. FRENCH	.550	9.1	73.1	73.6	+ 0.8	
9. GERMAN	.583	8.6	59.0	57.5	- 2.4	

differentiating gives the generation rate of optical absorption in the crystal. Thus, the generation g is

$$g = \alpha N_0 \, e^{-\alpha x} \tag{4}$$

and since α and N_0 are functions of wavelength then the generation function becomes

$$g(\lambda) = \alpha(\lambda) \, N_0 \, (\lambda) \, e^{-\alpha(\lambda) x} \tag{5}$$

For a defined incremental volume, it is intuitively apparent that under steady state equilibrium conditions the net rate of change in the minority carrier concentration must be equal to zero i.e., the generation within the incremental volume is equal to the rate of outward diffusion and the net recombination within the volume. The net rate of recombination is equal to the instantaneous electron density, which is $n-n_p$, divided by the lifetime, τ_n.

$$\text{recombination} = \frac{n - n_p}{\tau} \tag{6}$$

when considering an abrupt junction model and the flow of minority carriers solely by a diffusion process, the outward diffusion flow of current I_n is defined by

$$\text{diffusion} = \frac{1}{q} \frac{dI_n}{dx} \tag{7}$$

The outward current flow is also given by

$$\frac{I_n}{q} = D_n \frac{dn}{dx} \tag{8}$$

where

q = electronic charge
D = diffusion constant

Combining Eq 6 and 7 the diffusion component becomes

$$\text{diffusion} = D_n \frac{d^2 n}{dx^2} \tag{9}$$

Under steady state illumination the continuity equation is

$$\underset{\text{generation}}{\alpha(\lambda)\, N_0(\lambda)\, e^{-\alpha(\lambda)x}} = \underset{\text{recombination}}{\frac{n - n_p}{\tau}} + \underset{\text{diffusion}}{D_n \frac{d^2n}{dx^2}} \qquad (10)$$

Solutions to Eq. 10 have been programmed for varying solar cell parameters. An approximate solution is given by

$$\frac{I_n}{q} = \frac{N_0(\lambda)}{1 + \frac{1}{\alpha(\lambda)}}\, e^{-\alpha(\lambda)x}$$

which adequately describes the bulk current contribution of the solar cell.

In comparison to the collection efficiency of the surface region the bulk efficiency can clearly be established by the conventional techniques of the minority carrier diffusion model. The contribution of the total current density from the conventionally diffused n region is exceedingly complex and for large area solar cells the interrelation of the effects of surface recombination, a field induced contribution by virtue of the impurity profile, impurity scattering and general lack of accurate empirical data make the simple model somewhat nebulous.

A computer program has been formulated which enables the graphical comparison of empirical solar cell data from laboratory measurements and the solution of Eq. 10 for varying parameters of junction depth and diffusion length. Typical solutions are shown in Figures 14 through 18. Diffusion length measurements derived from the electron injection technique compares within 25 to 35% of the values obtained from the spectral response curves.

APPLICATIONS AND CONCLUSION

In addition to the most important application of the solar cell spectral measurement in calculating current densities for energy sources of known spectral irradiance there are applications in areas of solar cell materials improvement. By virtue of the minority carrier lifetime dependence of the absolute quantum yield any process or fabrication technique which modifies this bulk parameter can be readily documented by measuring the change in quantum yield as a function of the modifying mechanism. For particular crystallograph conditions in orientation, the junction formation process can be optimized by relating its effects to the resultant quantum yield. It is apparent that the spectral response measurement is readily applicable to any investigation of solar cell properties which involve the fundamental physical parameters.

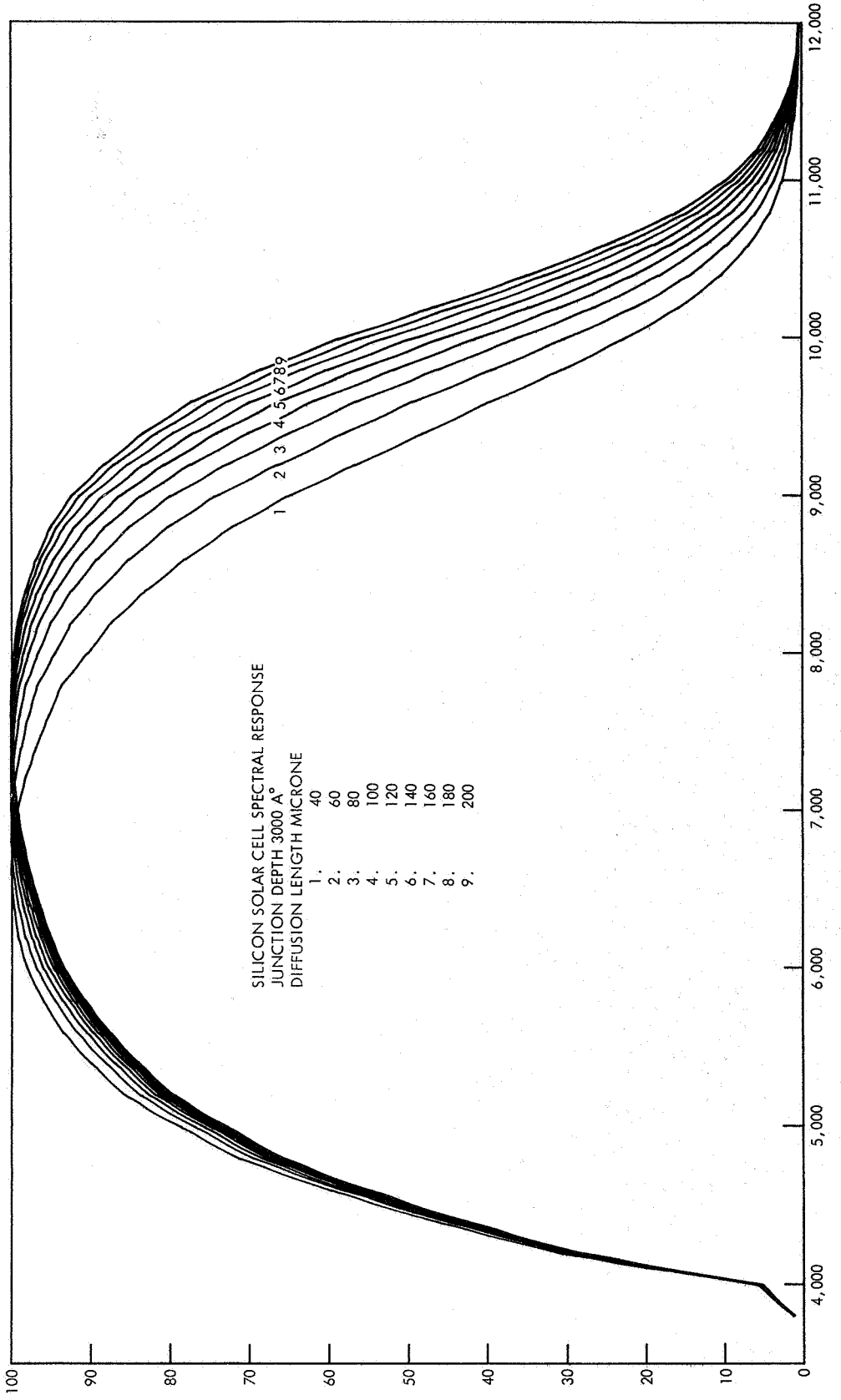

Figure 14. Solar Cell Spectral Responses

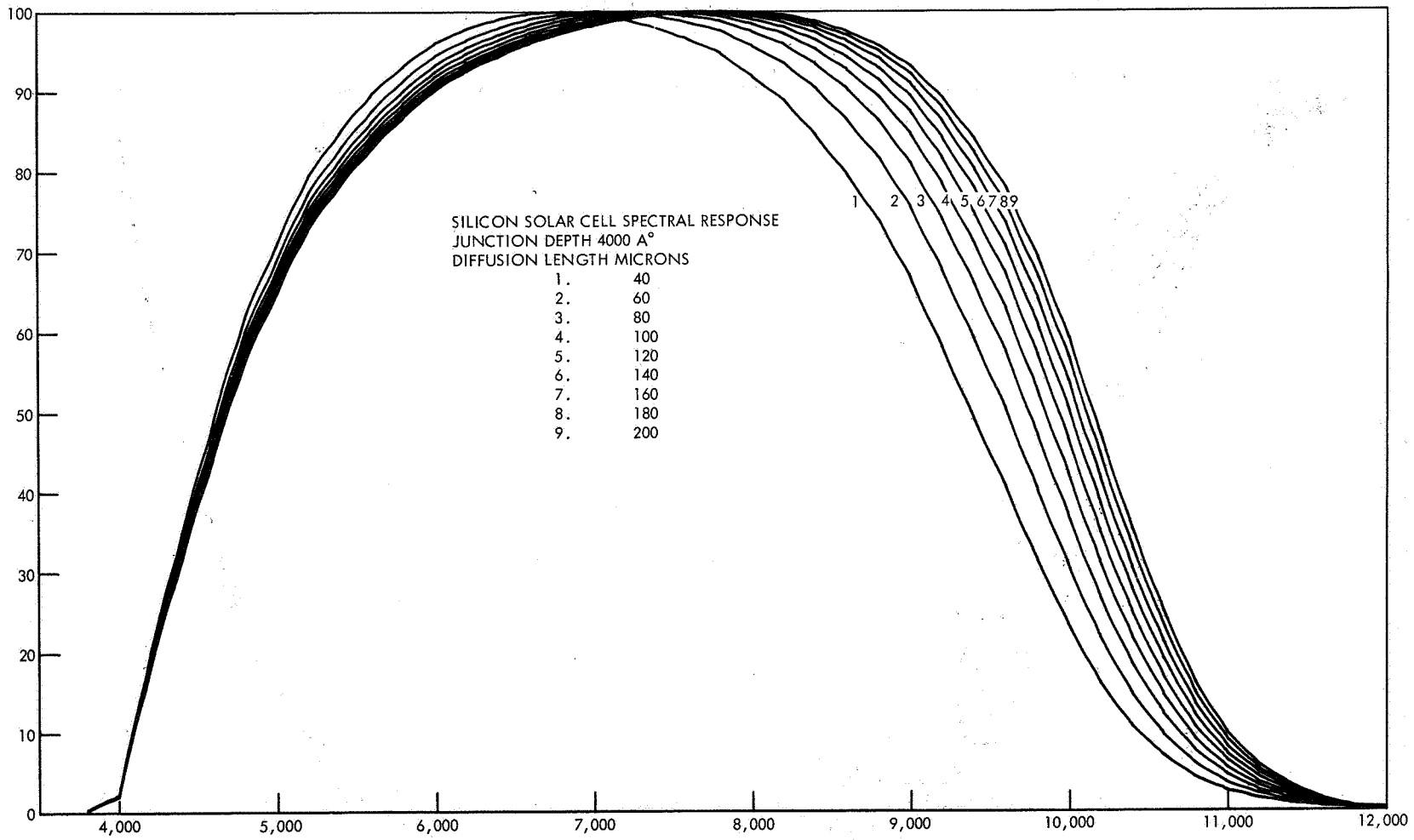

Figure 15. Solar Cell Spectral Responses

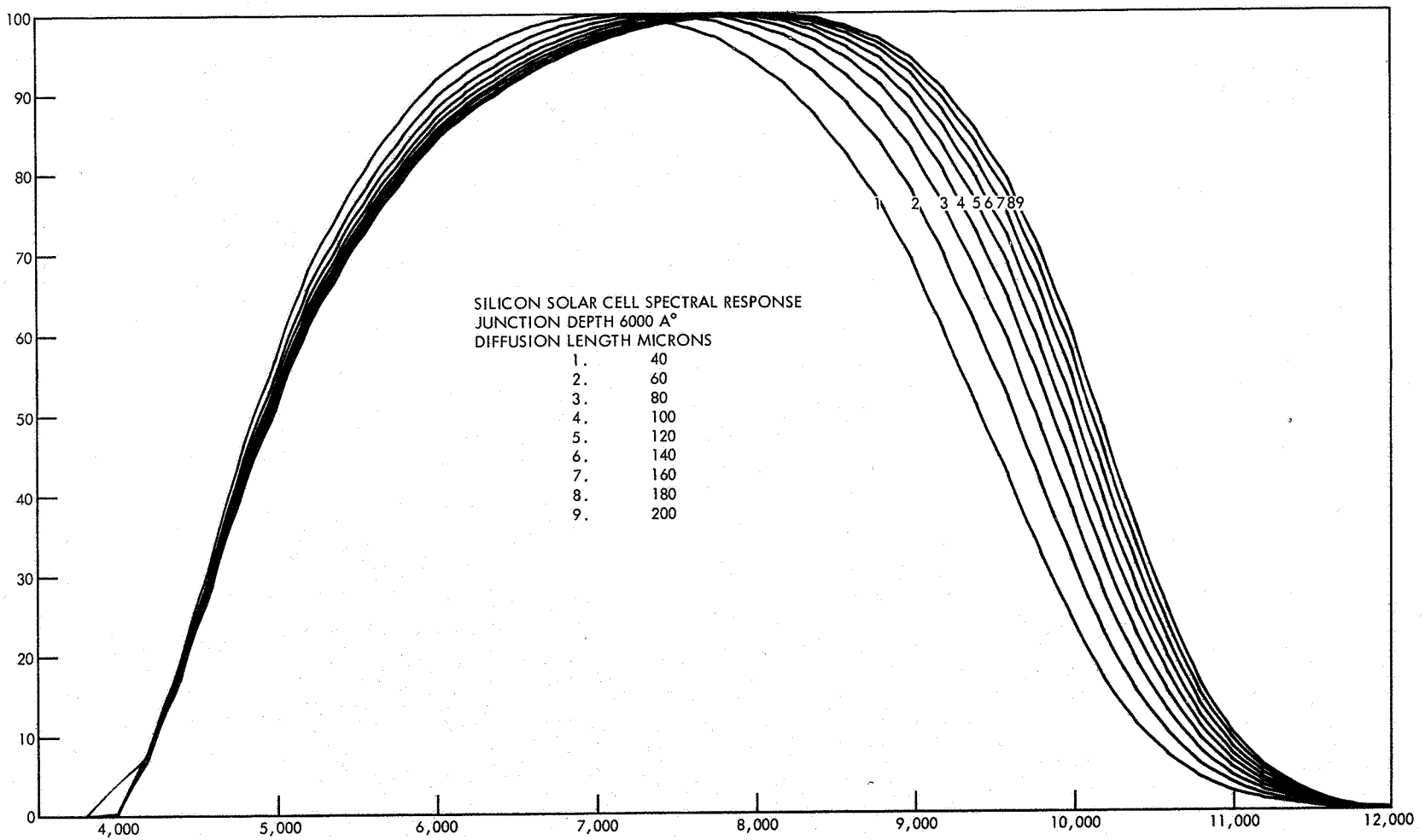

Figure 16. Solar Cell Spectral Responses

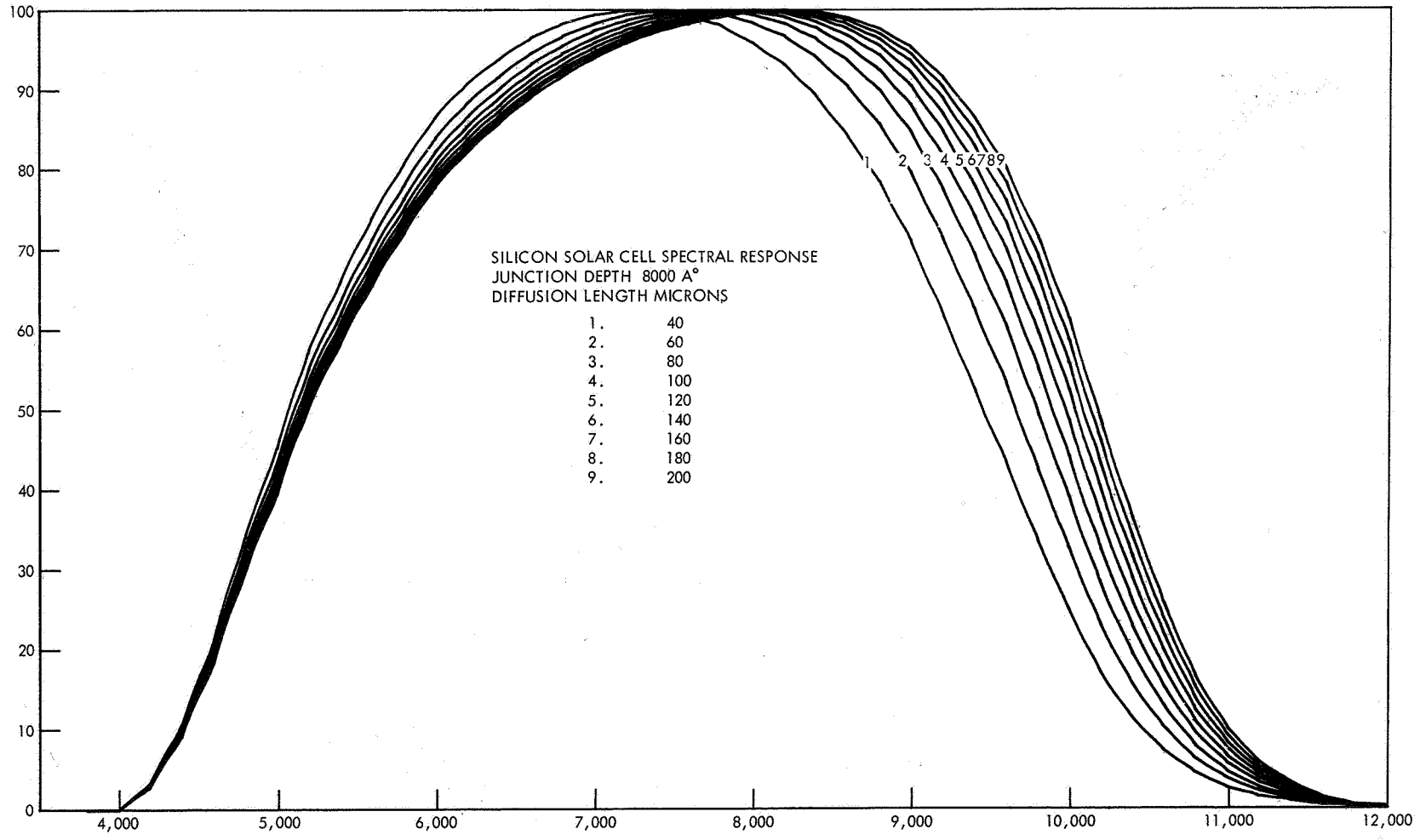

Figure 17. Solar Cell Spectral Responses

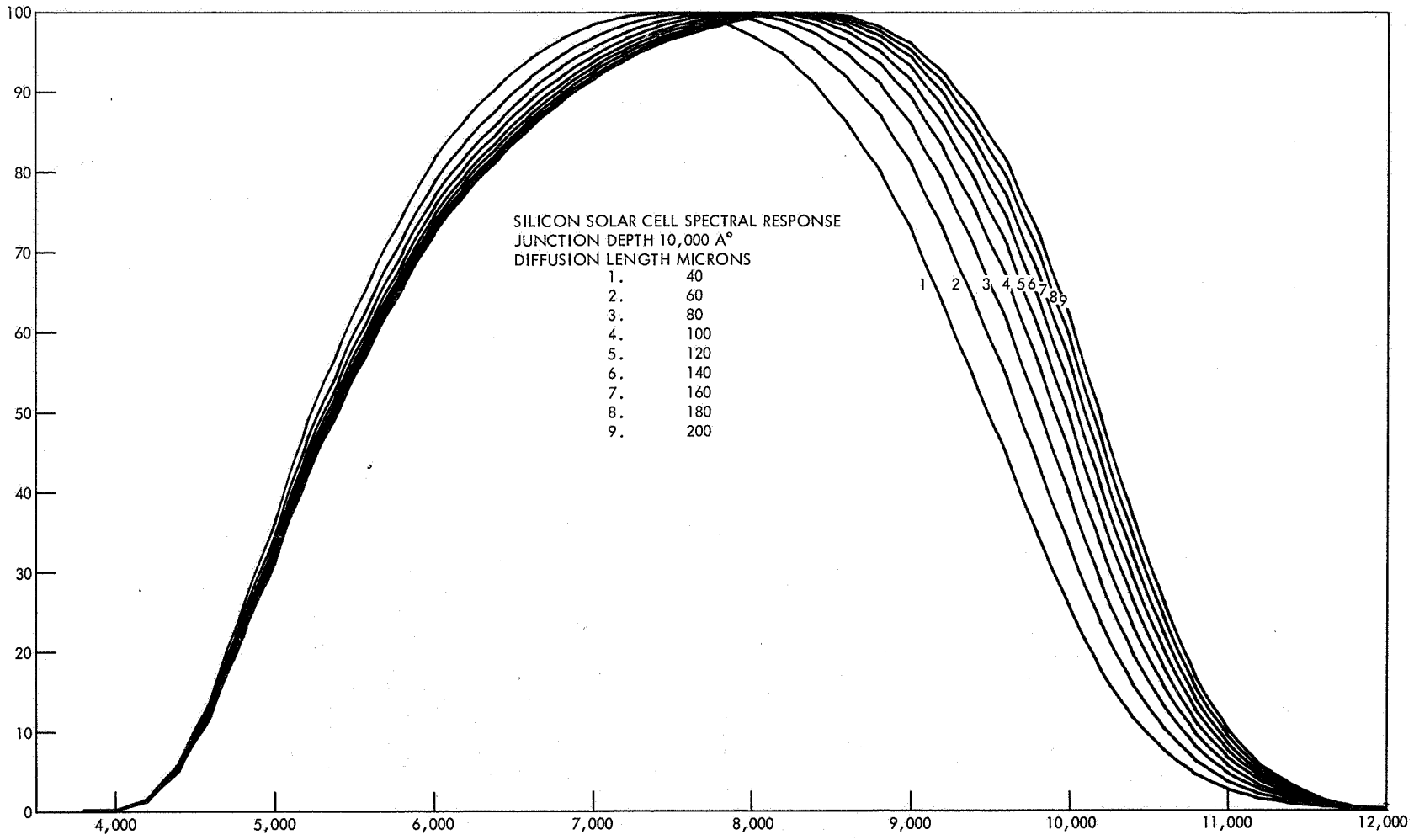

Figure 18. Solar Cell Spectral Responses